In Vivo Quantification and Parametric Images of the Cardiac β-Adrenergic Receptor Density

Jacques Delforge, PhD[1]; Didier Mesangeau, PhD[2]; Frédéric Dolle, PhD[1]; Pascal Merlet, PhD[1]; Christian Loc'h, PhD[1]; Michel Bottlaender, MD, PhD[1]; Régine Trebossen, PhD[1]; and André Syrota, MD, PhD[1]

[1]*Service Hospitalier Frédéric Joliot, Commissariat à l'Energie Atomique/Direction des Sciences du Vivant, Orsay, France; and* [2]*Merck–Lipha, Centre de Recherche de Chilly-Mazarin, Chilly-Mazarin, France*

Previous studies showed that the in vivo concentration of β-adrenergic receptor sites can be estimated by PET using (−)-4-((*S*)-3-tert-butylamino-2-hydroxypropoxy)-1,3-dihydrobenzoimidazol-2-one (CGP 12177), a hydrophilic ligand. A graphic method was previously proposed and used by several groups. However, this approach was not completely validated. The purpose of this study was to improve and confirm the validity of this approach through a better knowledge of the associated ligand-receptor model, estimated for the first time using the multiinjection approach. **Methods:** The concentration of β-adrenergic receptor sites was estimated for mini pigs using 2 methods. The first was the usual multiinjection approach, which permits estimation of all model parameters, including receptor concentration. However, this approach needs a complex protocol, including blood sampling, thereby making it difficult to use for studies on patients. The second method was the CGP 12177 graphic method. This approach permits the estimation of only receptor concentration but has the advantage of not requiring blood sampling. Another advantage is the ability to generate parametric images easily. **Results:** Using the multiinjection approach, we obtained for the first time a complete model describing interactions between CGP 12177 and β-adrenergic receptors. Knowledge of all parameters of this model permitted good validation of the assumptions included in the graphic method. The concentration of β-adrenergic receptor sites in mini pigs was estimated at 15.2 ± 3.4 pmol/mL. **Conclusion:** The graphic method has been improved by taking into account various phenomena, such as protein binding and the nonlinearity between plasma concentration and injected dose. This method is now usable for patient studies and offers the ability to estimate the β-adrenergic receptor concentration from a single PET experiment without blood sampling. Parametric imaging will enable screening of the receptor site location and observation of potential anomalies in patients.

Key Words: (−)-4-((*S*)-3-tert-butylamino-2-hydroxypropoxy)-1,3-dihydrobenzoimidazol-2-one (CGP 12177); β-adrenergic receptors; ligand-receptor modeling; parametric imaging

J Nucl Med 2002; 43:215–226

Quantification of cardiac β-adrenergic receptor sites is of significant interest for the study of heart diseases. There is ample evidence, from both experimental and clinical studies, that changes in β-adrenergic receptor density can be associated with cardiac diseases such as congestive heart failure, myocardial ischemia and infarction, cardiomyopathy, diabetes, or thyroid-induced heart muscle disease (*1–5*). Previous studies showed that (−)-4-((*S*)-3-tert-butylamino-2-hydroxypropoxy)-1,3-dihydrobenzoimidazol-2-one (CGP 12177) binds to myocardial β-adrenergic receptors with low and nonspecific binding in heart and lung tissue, thanks to both its high hydrophilicity and its affinity (*6–8*). Therefore, this molecule labeled with ^{11}C has been proposed to quantify β-adrenergic receptor sites in vivo (*9*).

In vivo estimation of the concentration of receptor sites is based on a mathematic model describing interactions between ligand and receptor sites. The parameters of the model are kinetic rate constants, except for 1 parameter that represents receptor concentration (B'_{max}). Many previous studies with various brain or heart molecules have evidenced the ability to identify all model parameters using a multiinjection approach, in which experimental protocols include several injections of labeled or unlabeled ligand (*10,11*). A first attempt to use the multiinjection approach with CGP 12177 on dogs failed because of a bad estimate of input function in the mathematic model (*12*). Indeed, the main difficulty of this approach is the need to measure the input function (usually the concentration of unchanged free ligand in the arterial plasma). Under certain conditions (nonmetabolized ligand, no binding to proteins, or a constant protein-binding percentage), this input function can be estimated directly from the PET-measured concentration in the cardiac cavity (*13,14*). However, binding of CGP 12177 to proteins depends on the injected mass and is a function of time; as a result, the input function cannot be estimated from the PET-measured concentration in the cavity. The multiinjection approach can be used with this molecule but requires blood sampling and is therefore difficult to implement for routine examinations on patients.

Consequently, a graphic method for estimating receptor concentration using CGP 12177 was previously proposed.

Received Mar. 26, 2001; revision accepted Sep. 25, 2001.

For correspondence or reprints contact: Jacques Delforge, PhD, Laboratoire de Radiotoxicologie, LRT/DSV, Commissariat à l'Energie Atomique, Centre d'Etudes de Bruyères-le-Châtel, BP 12, F-91680 Bruyères-le-Châtel, France.

E-mail: jacques.delforge@cea.fr

This approach, based on a 2-injection protocol and on a relationship between B'_{max} and some characteristics of the experimental curves (*12*), permits estimation of only 1 parameter—that is, concentration of β-adrenergic receptor sites—but offers the advantage of avoiding blood sampling. This method has been used by several groups of investigators in both heart (*15–17*) and lung (*18,19*) studies. However, it is based on several assumptions, which have to be validated. Because global knowledge of the model was lacking, validation of this graphic method was not completed.

Therefore, the first purpose of this study was to use the multiinjection method to obtain a model describing interactions between CGP 12177 and β-adrenergic receptor sites on mini pigs. A first estimate of the receptor concentration was thus obtained. Our second purpose was to modify and fully validate the CGP 12177 graphic method using the knowledge gained through this model. In particular, the B'_{max} values obtained with this simplified approach were compared with the receptor site concentrations estimated using the multiinjection method. Moreover, the simplicity and robustness of the proposed graphic method make it easy to estimate the receptor concentration pixel by pixel. Therefore, our third purpose was to obtain parametric images of β-adrenergic receptor site density. Such images make it possible to screen both the localization and quantification of receptor sites in the entire brain, thus providing an investigation tool for identifying possible local changes or anomalies in patients.

MATERIALS AND METHODS

Radiopharmaceutical Preparation

CGP 12177 was prepared as described previously (*20–22*). The total amount (in nanomoles) of injected radiolabeled CGP 12177 was adjusted to the desired value used in the PET protocol by adding a known quantity of unlabeled CGP 12177.

Animal Preparation

Male mini pigs (Yucatan Micropig; Charles River, St. Aubinles-Elbeuf, France) from 7 to 9 mo old were used. The animals were medicated in advance with acepromazine, 0.5 mg/kg intramuscularly. Anesthesia was induced and maintained by mask-induction isoflurane, 3% ± 0.5% in O_2/CO_2 (95%/5%). For venous blood withdrawals, a venous access port (Vygon Corp., East Rutherford, NJ) consisting of a reservoir and a catheter was inserted into the superficial jugular vein. For arterial blood samples, a catheter was implanted into the primary carotid artery. The hemodynamic parameters were monitored during the experiment to verify that they remained stable. All experiments complied with the relevant guidelines of the French Ministry of Agriculture for experimentation on animals and with the *Guide for the Care and Use of Laboratory Animals* (*23*).

Blood Sampling

Arterial blood samples were drawn into a heparinized Vacutainer (Becton, Dickinson and Co., Franklin Lakes, NJ) and were handled on ice. Two-hundred-microliter aliquots were weighted and counted for activity in a γ-well counter (Cobra; Packard Instrument Co., Inc., Downers Grove, IL). The blood samples were centrifuged (5 min, 3,000 rpm, 4°C) to obtain cell-free plasma, out of which 200-μL aliquots were weighted and counted for activity. The free fraction of ^{11}C-CGP 12177 in plasma was obtained by ultrafiltration, at 10 min, 3,000 rpm, and 4°C, on a 20,000-Da cutoff membrane (SM 13229; Sartorius, Goettingen, Germany). The radioactivity of the ultrafiltrate was measured in 200-μL samples.

To measure the amount of unchanged radiotracer in total plasma with high-performance liquid chromatography (HPLC), 200 μL plasma were mixed with 450 μL methanol containing 5 μg CGP (11 μg/mL) as the reference compound. After centrifugation (5 min at 3000*g* and 4°C), 0.5 mL of the supernatant was diluted with 0.05 mol/L Na_2HPO_4. To measure the amount of unchanged radiotracer in the free fraction, 200 μL of the deproteinized plasma were mixed with 0.3 mL 0.05 mol/L Na_2HPO_4 and with 450 μL methanol containing 5 μg cold CGP and were analyzed by radiolabeled HPLC as described above.

Ligand-Receptor Model

The compartmental model used in this study (Fig. 1) was based on the usual nonequilibrium, nonlinear model (*10,24–26*). It included 3 compartments (unchanged free ligand in plasma, free ligand in tissue, and specifically bound ligand) and 6 parameters (5 kinetic rate constants and B'_{max}, the total receptor site concentration available for binding). The nonspecific binding and the internalization phenomenon were assumed to be negligible.

The PET-measured concentration was the sum of the labeled ligand in the 2 tissue compartments and of a fraction F_V of the

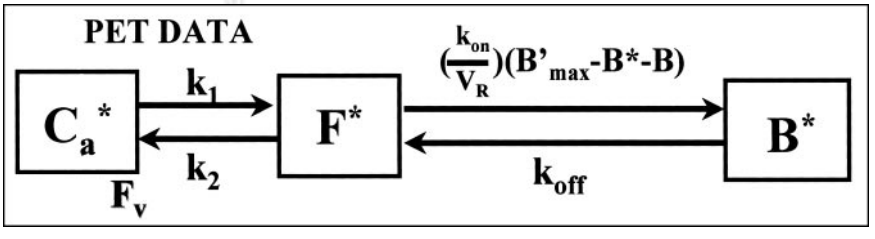

FIGURE 1. Three-compartment ligand-receptor model used for analysis of CGP 12177 time–concentration curves obtained with PET. All transfer probabilities of ligand between compartments are linear, except for binding probability, which depends on local association rate constant (k_{on}), on local free ligand concentration ($F^*(t)/V_R$), and on local concentration of unoccupied receptor sites (B'_{max}-$B^*(t)$). PET experimental data correspond to sum of labeled ligand in 2 tissue compartments and of fraction F_V of blood concentration. B and B* = unlabeled and labeled bound ligand concentrations, respectively; B'_{max} = receptor concentration; C_a^* and F* = free ligand concentration in blood and tissue, respectively; k_1 and k_2 = rate constants; k_{on} and k_{off} = association and dissociation rate constants, respectively.

blood concentration (which represented the blood volume in the tissue and the spillover effect).

Model Parameters Estimated Using Multiinjection Approach

The multiinjection approach consisted of performing several injections of labeled or unlabeled ligand, distributed throughout the study. In this study, 8 PET experiments were performed on mini pigs (Table 1). The experimental protocol included 3 injections infused intravenously for 45 s. The first was a tracer injection of ^{11}C-CGP 12177 at the beginning of the experiment (time $T_1 = 0$) with a high specific activity (approximately 55 MBq with a specific activity ranging from 3,700 to 68,450 MBq/μmol). The second was an injection of ^{11}C-CGP 12177 with a low specific activity (approximately 28 MBq with a specific activity ranging from 925 to 16,650 MBq/μmol) at time T_2, 30 or 40 min after the beginning of the experiment. The injected CGP 12177 mass ranged from 5 to 12 μg. The third was an injection of a large amount of unlabeled CGP 12177 (approximately 0.5 mg) at time T_3 (90 min), which led to a "displacement" of the labeled ligand. The total duration of the experiments was 130 min.

This method required measurement of the unmetabolized ^{11}C-CGP 12177 concentration and free ^{11}C-CGP 12177 concentration in plasma, which were used as the input function. During PET acquisition, 60 arterial blood samples were withdrawn at designated times. Blood and plasma radioactivity was measured in a γ-counter, and the time–activity curves were corrected for ^{11}C decay from the time of the first injection. Metabolism of CGP 12177 was assumed to be negligible. The plasma concentrations were corrected for protein binding to obtain the input function.

This protocol enabled estimation of all model parameters (6 parameters, including receptor concentration and vascular fraction) by fitting the PET experimental curves through a minimization of the usual weighted least squares cost function (*10,27*).

Estimation of Receptor Concentration Using Graphic Method

This graphic method enabled estimation of the β-adrenergic receptor concentration using CGP 12177 as a ligand and did not require blood sampling (*12*). Twenty PET experiments were performed on mini pigs. The experimental protocol included 2 injections. The first was a tracer injection of ^{11}C-CGP 12177 at the beginning of the experiment (time $T_1 = 0$) with a high specific activity (approximately 110 MBq with a specific activity ranging from 12,950 to 92,500 MBq/μmol). The injected dose was identified as D_1*. The injection mass was limited to 1.5 μg so that <15% of the β-adrenergic receptor sites would be occupied by the ligand. The second was an injection of ^{11}C-CGP 12177 with a low specific activity (approximately 220 MBq with a specific activity ranging from 3,219 to 23,125 MBq/μmol) at time T_2 (40 min). The injected dose was identified as D_2*. If the low specific activity was obtained by adding a dose of unlabeled ligand, this dose was called D_2. The doses were chosen so that 60%–80% of the receptor sites were occupied after the second injection. For mini pigs, the injected mass (including labeled and unlabeled CGP 12177) was limited to 7 μg.

This method was based on the fact that the myocardial time–activity curve covers 2 periods. The first is a distribution phase with fast kinetics for approximately 5 min after a high-specific-activity injection and for 10 min after a low-specific-activity injection. The second is a slow-kinetics period when the time–activity curve becomes a straight line: a plateau (or a slowly decreasing plateau) after the initial tracer injection and a slowly decreasing plateau after the second injection (with a higher injected mass). This method assumed that the free ligand concentration was negligible after the distribution phase. As a result, during the slow-kinetics periods (represented by a straight line), bound ligand concentration could be deduced directly from PET concentration after correcting for vascular fraction.

In the region-of-interest approach, the PET curves were corrected for vascular fraction by setting parameter F_V to 0.4, the blood concentration being estimated by the PET-measured concentration in the cavity. In the parametric imaging approach, the PET curves were corrected for vascular fraction pixel by pixel: The map of the vascular fraction was obtained by dividing the mean PET concentration during the first minute after the initial injection by the mean blood concentration measured in the cavity during the same period.

Two concentrations were deduced from the experimental data after correction for the vascular fraction: C_1*, which represented the level of the first plateau at the end of the distribution phase (5 min after injection), and C_2*, which represented the similar value obtained after the second injection. To account for the PET-measured radioactivity resulting from the first injection, C_2* was estimated from the level of the second plateau occurring at time $T_2 + 5$ by subtracting the concentration measured just before this

TABLE 1
Detailed Values of Experimental Protocols Used in the 8 Multiinjection Experiments

Experiment	Specific activity (at T_1) (GBq/μmol)	Dose D_1* (nmol)	Time T_2 (min)	Dose D_2* (nmol)	Time T_3 (min)	Dose D_3 (mg)	Total duration (min)
1	3.6	22.30	40	55.8	90	0.562	130
2	18.0	4.42	40	36.5	90	0.523	130
3	19.5	5.46	40	42.6	90	0.487	130
4	9.5	2.97	40	39.0	90	0.516	130
5	39.1	5.26	30	32.9	90	0.533	140
6	68.6	1.97	40	12.6	90	0.565	140
7	41.6	3.40	40	24.8	90	0.494	140
8	44.9	3.30	40	24.0	90	0.531	140

D_1*, D_2*, and D_3 are doses of CGP 12177 injected at times T_1 (=0), T_2, and T_3, respectively. Asterisk indicates that ligand is labeled.

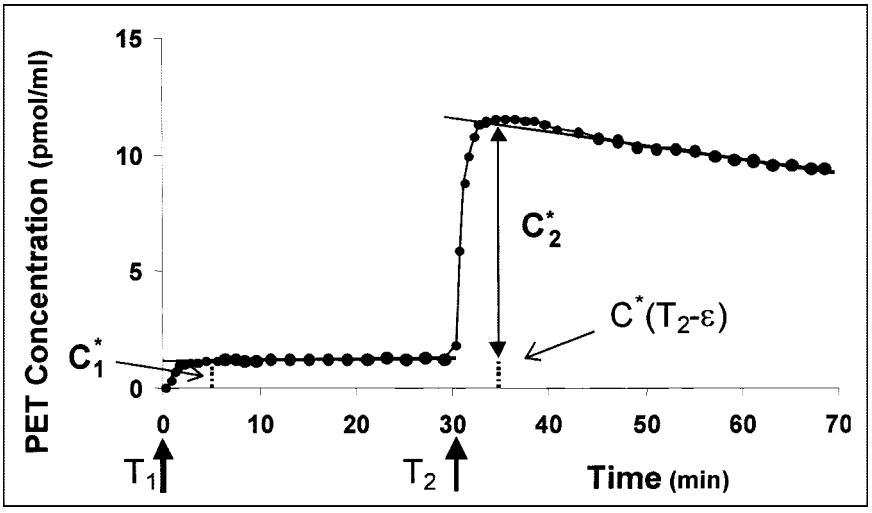

FIGURE 2. Estimation of β-adrenergic receptor density using graphic method. Experimental protocol includes 2 injections with doses D_1^* and D_2^* at times T_1 and T_2, respectively. Graphic method is based on measurement of 2 plateau levels at end of distribution phase (C_1^* and C_2^*). Plateaus are estimated from only portion of PET data (large ●), other data (small ●) being disregarded by graphic method. Receptor density is obtained from Equation 2. From current data (specific activity = 29,415 MBq/μmol, D_1^* = 3.09 nmol, D_2^* = 22.19 nmol) and using vascular fraction of 40%, receptor concentration is estimated at 18.6 pmol/mL.

second injection (which could be slightly different from C_1^* and thus was called $C^*(T_2 - \varepsilon)$; Fig. 2).

This method required information on the integral of the free ligand concentration during the distribution phase (Appendix). In the first study (*12*), the assumption was that this integral was proportional to the injected CGP 12177 dose. However, this assumption seemed invalidated by previous studies performed on humans, because the blood concentration apparently did not have a linear relationship to the CGP 12177 dose: After a low-specific-activity injection, the ratio of the blood concentration to the injected dose was significantly higher than the same ratio obtained after a high-specific-activity injection. Moreover, because of the association with red blood cells, the ratio between plasma and blood concentrations varied with time and was dependent on the injected mass. Therefore, a correction factor identified as α was introduced and was estimated from both the blood concentration measured in the cavity (denoted by $B_c^*(t)$) and the ligand doses, through the following relationship:

$$\alpha = \mu \frac{D_1^* \int_{T_2}^{T_2+\Delta} B_c^*(t)dt}{D_2^* \int_0^{\Delta} B_c^*(t)dt}, \qquad \text{Eq. 1}$$

where coefficient μ (set at 1.15, as described in the Results) enabled us to take into account the small difference in the association of CGP 12177 to red blood cells between the high and low specific activity (*28*).

Finally, the receptor concentration was derived from the solution to the following nonlinear equation (Appendix):

$$(B'_{max} - C^*_{(T_2-\varepsilon)})\left(1 - e^{\alpha\left(\frac{D_2 + D_2^*}{D_1^*}\right)\log\left(\frac{B'_{max} - C_1^*}{B'_{max}}\right)}\right) - C_2^* \frac{D_2 + D_2^*}{D_2^*} = 0. \qquad \text{Eq. 2}$$

In this equation, all values are known (D_1^*, D_2^*, and D_2 are ligand doses; C_1^*, C_2,* and $C^*(T_2 - \varepsilon)$ are estimated from the myocardial PET curve; and α is estimated from the cavity PET curve), except for B'_{max}, which appears twice. The unique solution to this equation, which is of the type "$f(B'_{max}) = 0$," can easily be obtained using a numeric or a graphic method.

PET Measurement and Data Analysis

All experiments using the multiinjection protocol were performed on an ECAT 953B positron tomograph (CTI, Knoxville, TN/Siemens Medical Systems, Inc., Hoffman Estates, IL) that was capable of acquiring 31 continuous slices simultaneously. Axial resolution was 5 mm (full width at half maximum), and spatial transverse resolution on the reconstructed images, with the Hanning filter, was 8.4 mm. Transmission scans were acquired with 3 rotating ^{68}Ge–^{68}Ga sources and were used to correct emission scans for the attenuation of 511-keV photon rays through the tissues. The experiment using the graphic method was performed both on the ECAT 953B positron tomograph and on an ECAT EXACT HR+ (CTI/Siemens) positron tomograph. This second tomograph was capable of acquiring 63 continuous slices simultaneously. The resolution in the 2-dimensional mode measured at 1 cm from the center was 4.5 mm in the transverse direction and 4.1 mm in the axial direction.

A 76-frame (multiinjection protocol) or a 51-frame (graphic method) dynamic emission scan was used to define the temporal and spatial distribution of the tracer in vivo. Time–activity curves were measured in regions of interest manually drawn on static 20-min images of 2 or 3 consecutive slices obtained 10 min after the first injection. The concentration of ^{11}C-CGP 12177, expressed in pmol/mL, was deduced from the ^{11}C activity concentration after correction for ^{11}C decay and after dividing by the specific activity, which was common to all labeled injections (because they resulted from the same synthesis). The data were corrected for partial-volume effect using echographic measurement of left ventricular wall thickness and a recovery coefficient factor measured experimentally using a heart phantom.

RESULTS

Blood Sampling and Input Function

Estimation of input function is an important step in the multiinjection approach, whereas study of the relationship between injected dose and blood time–concentration curve is required for the graphic approach (through estimation of the coefficient α). Our results confirmed that the metabolism

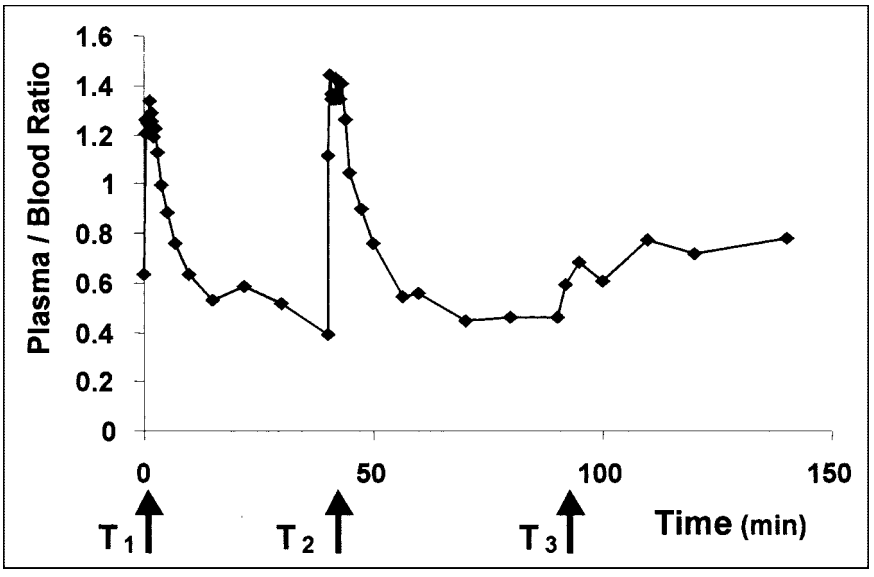

FIGURE 3. Example of plasma and blood ratio curves obtained with mini pigs using multiinjection protocol (Table 1, experiment 7, shows timing and injected doses). This ratio is not constant, in particular because of association of CGP 12177 with red blood cells.

of CGP 12177 in mini pigs is negligible: The mean percentage of metabolites obtained from 22 sample studies was <0.3%. Binding to the protein was estimated at 22% ± 4% of the plasma concentration, with no significant time variations or specific-activity effect. Therefore, for the multiinjection approach, the input function was estimated at 78% of the plasma concentration.

As previously reported by Van Waarde et al. (*28*) for humans, the association of CGP to red blood cells is significant and variable with time. Figure 3 shows the ratio of plasma concentration to blood concentration obtained in a multiinjection experiment (this example corresponds to experiment 7; Table 1 shows the doses). The integration of this curve during the first 5 min after injection was approximately 15% larger after the second injection (with a low specific activity) than after the initial tracer injection. This result accounted for the 1.15 value of coefficient μ. The injection of a large amount of unlabeled CGP 12177 after 90 min led to a significant increase in the ratio of plasma concentration to blood concentration, resulting from a small displacement of CGP 12177 molecules bound to red blood cells or other peripheral sites.

Using Equation 1, the coefficient α was estimated at 2.01 ± 0.27 using blood sampling and 1.85 ± 0.20 using the PET-measured concentration in the cavity. In other words, without this α correction, the level of the second plateau, C_2*, would be overestimated by a factor of close to 2.

Results of Multiinjection Approach

Eight multiinjection experiments with blood sampling were performed. Table 1 gives the detailed protocols, with timing and doses, and Table 2 gives the model parameters estimated in each experiment.

Figure 4 shows an example of a PET time–concentration curve obtained for myocardium using the multiinjection protocol (experiment 7; Table 1 shows the doses). The shapes of the curve after the first 2 injections are similar to

TABLE 2
Detailed Results of Model Parameters Estimated from the 8 Multiinjection Experiments

Experiment	B'_{max} (pmol/mL)	k_1 (min^{-1})	k_2 (min^{-1})	k_{on}/V_R (mL/[pmol min])	k_{off} (min^{-1})	F_V	K_dV_R (pmol/mL)
1	17.5	0.32	6.1	0.74	0.020	0.47	0.027
2	11.6	0.72	4.0	0.85	0.020	0.57	0.023
3	11.5	0.80	1.7	0.68	0.022	0.20	0.036
4	8.8	0.57	1.2	0.51	0.018	0.25	0.035
5	17.4	1.32	2.2	0.33	0.015	0.78	0.046
6	12.1	0.81	1.3	0.30	0.019	0.39	0.063
7	10.0	0.58	2.1	0.76	0.018	0.52	0.024
8	12.9	0.96	3.1	0.58	0.016	0.20	0.028
Mean	12.7	0.76	2.7	0.59	0.018	0.42	0.035
SD	3.2	0.30	1.7	0.20	0.002	0.20	0.013

Table 1 shows doses used. Model parameters are defined in Figure 1 legend.

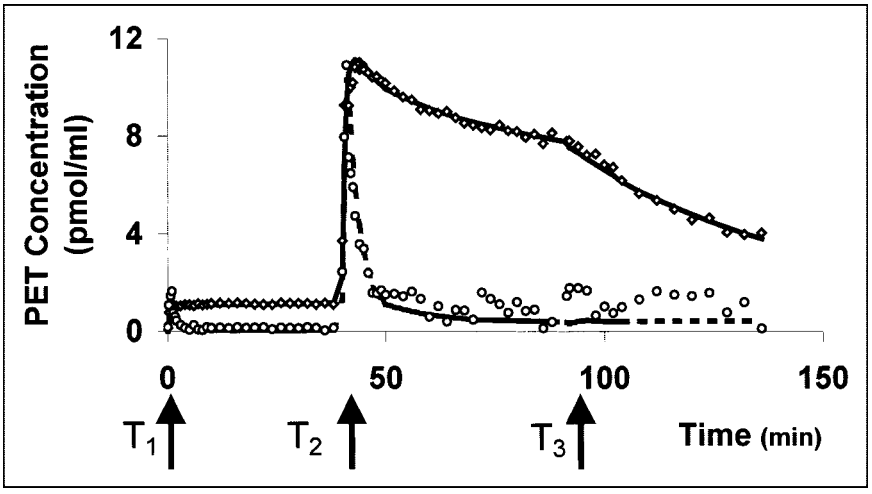

FIGURE 4. Example of PET time–concentration curves obtained with mini pigs using multiinjection protocol. Experimental data obtained in experiment 7 (Table 1 shows timing and injected doses) in myocardium are represented by ◇. Solid line, which is simulated curve obtained from estimated model parameters (Table 2), is close to experimental data. This proves quality of fit obtained using 3-compartment model. PET-measured concentrations in cavity (○) are good estimates of blood concentration measured by sampling (dotted line) during first 10 min after injection. After this period, low concentration and heart movements lead to noisy data.

the shapes obtained with the graphic-method protocol, with a plateau after the first tracer injection and a straight line slowly decreasing approximately 12 min after the low-specific-activity injection. The last injection—of a large amount of unlabeled ligand—leads to a displacement phenomenon. The figure shows the quality of the fitting procedure (experiment 7; Table 2 shows the values of the parameters) because the simulated curve appears close to the experimental data. The peak after each injection occurs quickly, whereas blood concentration drops approximately 10 min after each injection. The cavity PET concentration appears to be a good estimate of the blood concentration for approximately 10 min after the injection. Thereafter, however, the low concentration levels and heart movements make for noisy data.

The multiinjection approach enabled simulation of the concentration in each compartment, because all model parameters were estimated (Table 2). In Figure 5 (corresponding again to experiment 7), the PET concentration is the sum of the concentration in the free and the bound compartments and of a fraction F_V of the blood concentration. During the first plateau, most of the labeled molecules were bound to the receptor sites (95%–98%) and the free ligand concentration was negligible. At time T_2, the second injection was a labeled CGP 12177 injection (dose D_2*) with a low specific activity, and thus, the percentage of receptor sites occupied by the ligand quickly reached approximately 85% (in the other experiments, this percentage ranged from 60% to 85% depending on the injected dose, reaching as much as 97% for experiment 1 in an extreme case). Consequently, the binding of the free ligand was less easy and, thus, its concentration was significant during approximately 10 min after injection. The higher the injected dose, the larger the free ligand concentration and, thus, the higher the peak observed approximately 3 min after injection. However, after this 10-min period, the free ligand concentration dropped to negligible levels, with most of these free molecules being returned to the blood circulation. Therefore, after time T_2 + 10 min, the PET concentration was again close to the bound ligand concentration, whereas the vas-

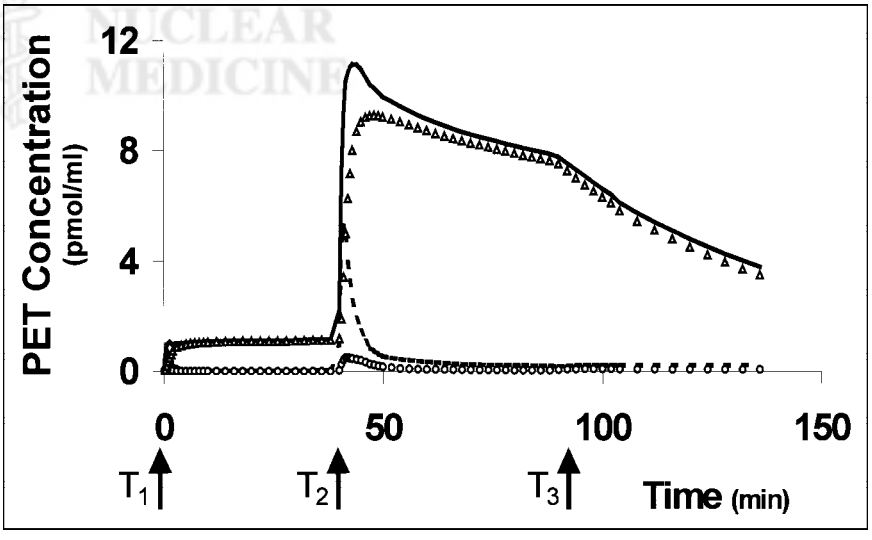

FIGURE 5. Simulations of CGP 12177 kinetics performed with model parameters estimated during experiment 7 (Fig. 4). Symbols represent concentrations in free (○) and bound (△) ligand compartments. Solid line represents PET-measured concentration that is sum of concentration in the 2 tissue compartments and of fraction F_V of blood concentration (dotted line, which represents in this case 52% of blood time–concentration curve shown in Fig. 4).

cular fraction represented only several percentage points of the PET-measured concentration. As the bound ligand concentration decreased slowly, the PET curve became a straight line with a small slope. Injection of an excess of unlabeled CGP 12177 (dose D_3 at time T_3) led to displacement of the bound labeled ligand by the unlabeled molecule. With the injected dose (0.5 mg), the displacement intensity reached its maximum, because this dose contributed to the saturation of all the receptor sites (98.7%). Consequently, this last slope of the curve is directly related to the dissociation parameter k_{off}.

Results of Graphic Method

Figure 2 shows a typical PET curve obtained using the graphic method. The plateau after the initial tracer injection starts after a time ranging from 3 to 8 min and estimates the C_1* value (the value of the straight line at 5 min). After the second injection, with a smaller specific activity, the straight line is obtained at approximately 15 min, which was the period required for the free ligand to disappear (Fig. 5). Therefore, the straight line was estimated using the PET data obtained during 45–70 min (Fig. 2; large ●). This permitted estimation of C_2*, which represented the difference between the PET-measured concentration at $T_2 + 5$ and the concentration measured just before this second injection ($C^*(T_2 - \varepsilon)$).

No significant change to the mini pigs' heart rate was observed during continuous monitoring, even after injection of the largest amounts of CGP 12177.

The influence of the vascular fraction in the PET-measured concentration was significant during the first few minutes after injection (Fig. 5; dotted line) but was low during the intervals used to estimate the plateau line. In the graphic method, the vascular fraction was not identifiable from the experimental data. Therefore, the correction for the vascular fraction was based on the parameter F_V set at 0.40, which was the mean value estimated from the multiinjection approach (Table 2). To test the uncertainties related to this assumption, we estimated the receptor concentration from the data represented in Figure 2 using F_V values ranging from 0 to 0.7. Without correction ($F_V = 0$), the B'_{max} estimate was 19.26 pmol/mL, which represents a 3.3% overestimate of the value obtained with $F_V = 0.4$ (18.64 pmol/mL). With the largest F_V value (0.7), the receptor concentration was estimated at 18.18 pmol/mL, which is a 2.5% underestimate.

The value of μ used in Equation 1 was not estimated for each experiment and was set to 1.15. However, our numeric simulations showed that the uncertainty about this parameter had only a small effect on the estimate of receptor concentration. For example, if the difference in the association of CGP 12177 to red blood cells between high and low specific activity was underestimated by 50% ($\mu = 1.10$), the biases on the receptor concentration ranged from 0.1% to 3%, with a mean of approximately 1%.

From the results obtained for 20 different mini pigs, the β-adrenergic receptor concentration was estimated at 15.2 ± 3.4 pmol/mL in the myocardium. A regional study led to a B'_{max} value estimated at 15.0 ± 3.5 pmol/mL in the lateral region, 14.3 ± 2.9 pmol/mL in the anterior region, and 15.9 ± 3.5 pmol/mL in the septal region.

Comparison of the 2 Receptor Density Estimates

The graphic method could be applied to the PET data resulting from the multiinjection protocol when restricted to only the first 2 parts of the curve. Table 3 compares the receptor concentrations estimated by the 2 methods. The results obtained with the exact graphic method are displayed in the last column of Table 3 (the vascular fraction was set to 0.4 and the blood concentration was the PET-measured concentration in the cardiac cavity). The results of the 2 methods were correlated ($P = 0.0002$; $r = 0.92$) and the estimates of mean receptor concentration were close: 12.7 ± 3.2 pmol/mL with the multiinjection approach versus 13.1 ± 2.7 pmol/mL with the graphic approach.

Because blood sampling was performed during the multiinjection experiment, we also tested the graphic method using these data so as to estimate the impact of various approximations. In the first column of graphic method results in Table 3, the correction for vascular fraction was performed using sampling of the blood concentration, whereas the correction factor α was estimated (from Equation 1) using plasma concentration (and thus without correction for red cell binding; $\mu = 1$). In contrast, in the second column of graphic method results, α was estimated using sampling of the blood concentration and therefore was corrected for red cell binding ($\mu = 1.15$). The estimates of the receptor concentration using these methods (which included fewer assumptions) were close to the values derived from the exact graphic method, given in the last column. These results support the validity of the correction for red cell binding and of the use of PET measurement in the cavity.

Parametric Imaging

One of the primary advantages of the graphic method lies in the ease of the calculations, enabling an easy pixel-by-pixel estimation of the receptor concentration and thereby offering the ability to generate parametric images. This parametric approach requires estimation of the vascular fraction, which is obtained pixel by pixel from the ratio between the mean PET-measured concentration in each pixel and the mean blood concentration measured in the cavity during the first minute. This method is based on the assumption that blood circulation is not much affected by transfers into the tissue during this short period. Figure 6 is an example of a vascular fraction image estimated by this method (the experiment is the same as for Fig. 2). The cavities appear clearly, with a vascular fraction close to 1. Because the blood concentration in the cavity is estimated using a large region of interest, F_V is expectedly a bit greater than 1 in several pixels.

TABLE 3
Receptor Concentration Estimated Using Kinetics and Graphic Approaches on Data Obtained from the 8 Multiinjection Experiments

Parameter	Multiinjection method	Graphic method		
		First estimation type	Second estimation type	Third estimation type
Vascular fraction				
F_V value	Estimated	0.4	0.4	0.4
Function used	Blood sampling	Blood sampling	Blood sampling	PET measurement in cavity
Input function/corrections				
Protein binding	22%	—	—	—
μ (red cells)	—	—	1.15	1.15
Function used	Plasma sampling	Plasma sampling	Blood sampling	PET measurement in cavity
Receptor concentration				
Experiment 1	17.5	15.8	15.7	16.0
Experiment 2	11.6	11.2	10.9	10.7
Experiment 3	11.5	11.6	11.5	11.5
Experiment 4	8.8	9.6	9.6	9.7
Experiment 5	17.4	17.4	18.2	17.6
Experiment 6	12.1	15.4	14.1	12.9
Experiment 7	10.0	13.2	11.5	12.3
Experiment 8	12.9	15.2	14.1	14.5
Mean	12.7	13.7	13.2	13.1
SD	3.2	2.7	2.8	2.7

Table 1 shows doses used. Receptor concentration is in pmol/mL. Detailed results of multiinjection approach are given in Table 2.

Figure 7 is an example of a quantified image of β-adrenergic receptor concentration obtained with the graphic method. The receptor concentration was estimated pixel by pixel without filtering and without correction for partial-volume effect. This figure shows the regional distribution of β-adrenergic receptors in the myocardium and septal region. The image is homogeneous, with good patterns. The receptor concentration is insignificant (<3 pmol/mL) outside the heart. The good quality of this image is evidence that the graphic method is robust and not too sensitive to PET uncertainties. This result is not surprising, because the experimental data (C_1* and C_2*) used in the graphic method result from a fit (by a linear function) of a large number of PET measurements.

DISCUSSION

Many groups have quantified the β-adrenergic receptor sites using the graphic method (*15–19*). The validity of this method has been supported, in both heart and lung studies, by the good correlations between B'_{max} estimates obtained by in vitro methods and by the current in vivo method (*15,18*). However, some unacceptable results obtained on patients (P. Merlet, unpublished data, 1995)—results showing large variations and including some large, unrealistic concentration estimates—indicate that this method may be subject to criticism. We performed this study on mini pigs to validate all the used assumptions. The rationale for using mini pigs lies in the similarity of their metabolism to that of humans and the possibility of using a multiinjection approach with blood sampling (thus permitting estimation of all model parameters describing interactions between the β-adrenergic receptor and CGP 12177).

The graphic method is based on 3 assumptions related to the kinetics of the ligand. The first assumption is that after the distribution phase, the PET-measured concentration (corrected for vascular fraction) is a good estimate of the bound radioligand concentration. The multiinjection approach validates this assumption, as is illustrated by Figure 5, which shows that the free ligand concentration was negligible after the distribution phases (<0.02% after the tracer injection and <0.5% after the low-specific-activity injection).

The second assumption states that the dissociation rate constant is sufficiently low for the dissociation reaction to be disregarded during the distribution phase. This assumption is supported by the parameter value estimated using the multiinjection approach ($k_{off} = 0.018 \pm 0.02\ min^{-1}$) and is required so that the effect of dissociation during the distribution phase may be disregarded, thus permitting analytic equations (Appendix). Simulations showed that the bias on B'_{max} resulting from this second assumption was <2%.

The last assumption is that the integral of the free ligand concentration during the distribution phases can be linearly related to the injected doses using a correction factor α. This hypothesis is important so as to avoid blood sampling (Appendix). Coefficient α is defined such that this hypothesis is verified (Eq. 1).

The metabolism of CGP 12177 was formerly controversial (*12,28–30*). Three problems were studied: the metabolism of CGP 12177, binding to proteins, and binding to red

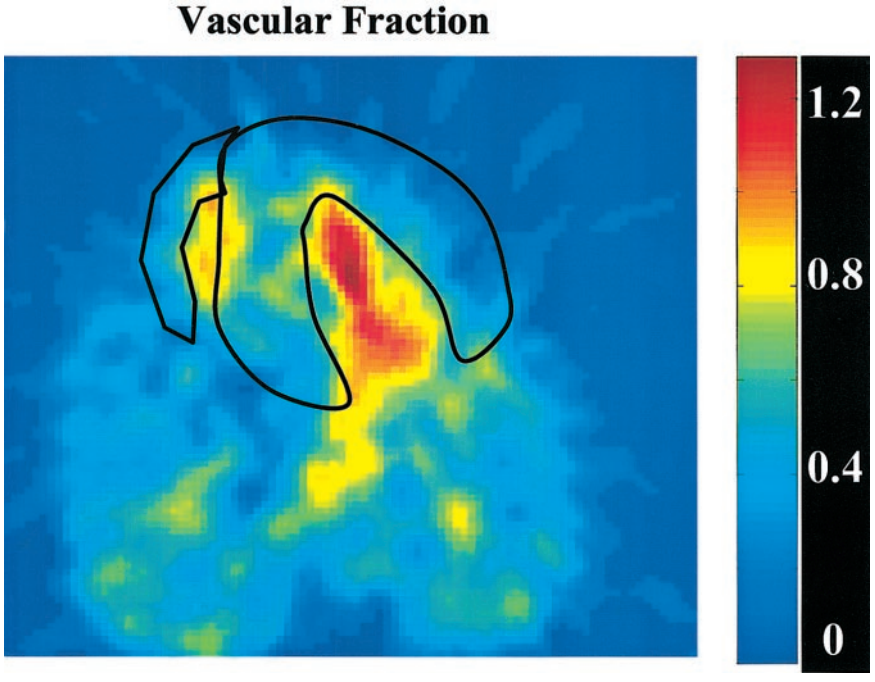

FIGURE 6. Example of vascular fraction image estimated pixel by pixel. For each pixel, vascular fraction is estimated by dividing mean PET concentration during first minute after first injection by mean blood concentration measured in cavity during same period. Limits of high-receptor-density area observed in Figure 7 are marked by line. Highest vascular fraction is observed in heart cavities.

blood cells. Most studies now agree in their conclusion that rats metabolize this molecule slowly whereas humans do not metabolize it to any significant extent (*28*). The same conclusion is obtained with mini pigs, in whom metabolism of this molecule is found to be negligible (<0.3%). Plasma protein binding is low for rats (30% ± 2%) and healthy human volunteers (31% ± 2%), these values being obtained instantaneously with no detectable change after injection (*28*). For mini pigs, plasma protein binding is also independent of time and is estimated at 22% ± 4%. Some studies evidenced an important association between CGP and red blood cells, possibly with small differences between low- and high-specific-activity injections (*28*). An exact correction for this phenomenon would require blood sampling for each experiment. However, the absolute percentage of binding to red blood cells has no influence on α (because α is defined by a ratio). As a consequence, it is sufficient to estimate the coefficient μ, which corrects the effect result-

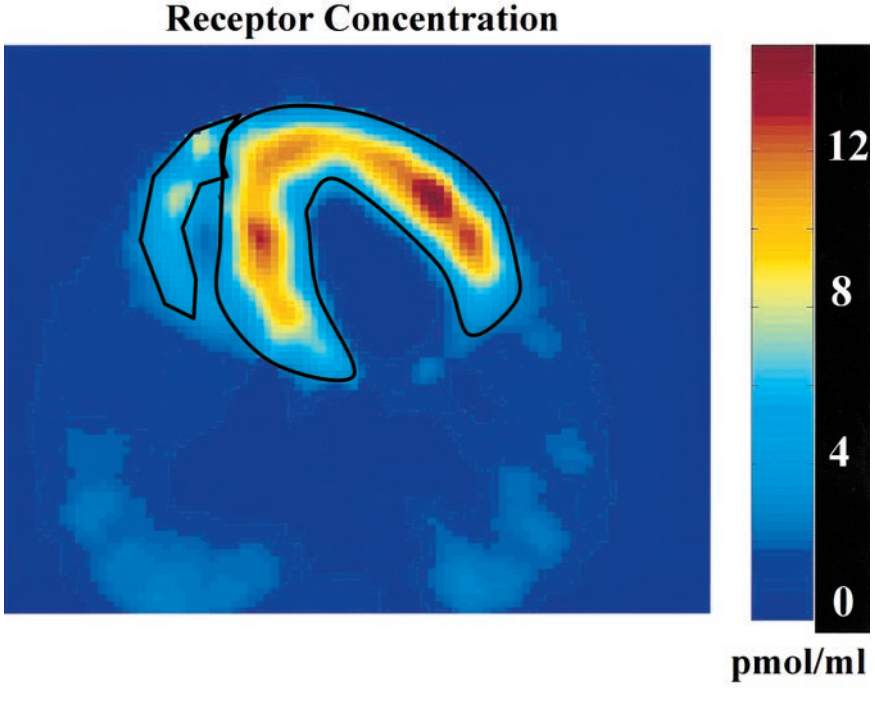

FIGURE 7. Example of parametric image of β-adrenergic receptor concentration. Experiment is same as in Figure 2 (legend of Fig. 2 describes doses). This image has been obtained by calculating receptor density using Equation 2, pixel by pixel and without filtering. Correction for vascular fraction is performed using Figure 6 results. No correction for partial-volume effect was performed.

ing from the different specific activities between the 2 injections. For mini pigs and the doses suggested by the graphic method protocol, the ratio of plasma concentration to blood concentration is approximately 15% higher during the first 10 min after the second injection than for the first injection. This percentage is in line with the results of Van Waarde et al. (*28*) obtained in humans. Therefore, the effect of binding to red blood cells is not measured in each experiment and is corrected using the value of μ (1.15) estimated from the multiinjection experiments. The biases resulting from this approximation appear acceptable (approximately 1%). Moreover, this correction is weak in comparison with the second and main phenomenon included in the correction factor α, that is, the nonlinearity between the injected doses and the blood concentration. This last phenomenon, which is corrected in each experiment from the PET-measured concentration in the cavity, accounts for approximately 85% of the α value (estimated for mini pigs at 2.0 ± 0.3).

This vascular fraction parameter, F_V, which includes blood volume and spillover effects, is estimated at 0.42 ± 20 using the multiinjection approach. The SD is large (this parameter is difficult to identify with CGP 12177 because of its fast blood kinetics), but this estimate is close to the value previously obtained with the same method and methylquinuclidinyl benzilate as ligand: 0.40 ± 10 for dogs (*13*) and 0.48 ± 0.14 for humans (*31*). This vascular fraction parameter cannot be estimated from the experimental data obtained using the graphic method protocol. Some groups suggested correcting the PET data for vascular activity and spillover by measuring tissue density and blood volume through a $C^{15}O$ experiment (*16,17*). However, this elaborate method needs venous samples and requires an additional PET experiment with a higher radiation dose and the usual risk that artifacts will be caused by movement between the 2 scans. Our results showed that the correction for vascular fraction is low for mini pigs (Fig. 5), and simulations showed that the receptor concentration estimate was not significantly biased by uncertainty about F_V (e.g., the bias was only 3.3% with no vascular fraction correction, as described in the Results) and by the noisy PET measures in the cavity. Therefore, it is acceptable to correct the vascular fraction using the F_V value set at 0.40 and the blood concentration measured in the cavity, because the bias resulting from uncertainties about these values can be deemed to be always $<2\%$.

The β-adrenergic receptor concentration in the mini pig myocardium was estimated at 12.7 ± 3.2 pmol/mL from the 8 multiinjection experiments (Table 2) and 15.2 ± 3.4 pmol/mL from the 20 experiments using the graphic methods.

These results can be compared with the values previously published: 11.5 ± 2.2 pmol/mL (*15*) and 6.6 ± 1.2 pmol/mL (*17*) for a healthy human and 30.9 ± 3.7 pmol/mL (*12*) for dogs. However, this comparison is perhaps irrelevant, because all these estimates were based on the graphic method and did not include correction for the nonproportionality between the injected dose and the model input function that is considered by α. This coefficient estimated for mini pigs, 2.0 ± 0.3, appears to be an important correction compared with the value of 1 previously used. However, the relationship between α and the estimate of B'_{max} is not obvious and varies as a function of the used doses. If the second injected dose, D_2^*, is large (and thus leads to quasicomplete occupancy of the receptor sites), the theory shows that the α value has no influence on the receptor density estimate, whereas simulations proved that the lack of correction factor α explains the large variability of results previously obtained for patients with doses leading to a receptor occupancy percentage $< 50\%$.

The graphic method offers the great advantage of permitting parametric imaging. Assessment of spatial distribution of receptor density by parametric imaging requires high-quality data and a robust method for pixel-by-pixel quantification. The example of a quantified image of β-adrenergic receptor concentration given in Figure 7 shows a homogeneous concentration in the myocardium. Obviously, the lack of correction for partial-volume effect explains the side effect and leads to an underestimation of receptor sites: The mean concentration in the myocardium is estimated at 18.6 pmol/mL (Fig. 2), whereas the maximum concentration observed in Figure 7 is 15 pmol/mL. However, such an image is useful for locating and quantifying potential anomalies in receptor concentration. The concentrations outside the heart are low, but only the order of magnitude of these estimates is valid, because an exact estimation of the β-adrenergic receptor—for example, in the lung—would require correction for tissue density (*18,19,32*).

Because this image was obtained without filtering, the homogeneity of the concentration estimated pixel by pixel proves the robustness of the method with little sensitivity to PET measurement uncertainties. This property results from the fact that the PET data are the coefficients C_1^* and C_2^*, which are obtained by fitting the PET data acquired over 20 or 30 min. Consequently, the bias on the estimation of receptor concentration results mainly from the other experimental data introduced in the model, such as specific activity, the estimate of α, and the correction for partial-volume effect.

CONCLUSION

Using the multiinjection approach, we obtained the first complete model describing the interactions between CGP 12177 and β-adrenergic receptors. Knowledge of all the parameters in this model provided a good validation of the assumptions included in the previously proposed graphic method. The main advantage of this graphic approach is that the results are obtained without having to measure the input function, that is, without having to estimate metabolites and protein binding. Another advantage is the ability to offer parametric images of receptor concentration and vascular

fraction. This property is important because it permits screening of receptor site localization and observation of possible anomalies in patients.

APPENDIX

Proof of Equation 2, Permitting Graphic Determination of Receptor Density

Introduction and Assumptions. This method is based on the fact that the myocardial time–activity curve becomes a straight line approximately 10 min after injection of CGP 12177. Therefore, in the myocardial PET curve, one can distinguish an initial distribution phase (approximately 5 min after injection, with this delay being denoted by Δ), followed by a slow kinetic period (represented by a straight line). This method is based on 3 assumptions. Assumption 1 is that after the distribution phase, the measured PET concentration, corrected for vascular fraction, represents the bound ligand concentration (the free ligand concentration and the nonspecific binding are negligible). Assumption 2 is that the dissociation rate constant is low enough for the dissociation phenomenon during a fast kinetic period to be disregarded. Assumption 3 is that the integral of free ligand concentration during distribution phases can be linearly related to injected doses using a correction factor called α.

Definition and Calculation of α. Assumption 3 states that the relationship between free ligand concentration and ligand dose after the first injection is defined by:

$$\int_0^{\Delta} F^*(t) = \gamma D_1^*, \qquad \text{Eq. 1A}$$

whereas the relationship associated with the second injection is given by:

$$\int_{T_2}^{T_2+\Delta} F^*(t) = \alpha\gamma D_2^*. \qquad \text{Eq. 2A}$$

Therefore, the correction factor α is defined by:

$$\alpha = \frac{D_1^* \int_{T_2}^{T_2+\Delta} F^*(t)dt}{D_2^* \int_0^{\Delta} F^*(t)dt}. \qquad \text{Eq. 3A}$$

To estimate this parameter in practice, the validity of the following relationships is assumed:

$$\frac{\int_{T_2}^{T_2+\Delta} F^*(t)dt}{\int_0^{\Delta} F^*(t)dt} = \frac{\int_{T_2}^{T_2+\Delta} C_a^*(t)dt}{\int_0^{\Delta} C_a^*(t)dt} = \mu \frac{\int_{T_2}^{T_2+\Delta} B_a^*(t)dt}{\int_0^{\Delta} B_a^*(t)dt}, \qquad \text{Eq. 4A}$$

where $C_a^*(t)$ is the free ligand concentration in the plasma (the input function) and $B_a^*(t)$ is the ligand concentration in the blood. The coefficient μ makes it possible to account for the effect of the difference in binding to red blood cells related to the different specific activities, as described in the text. Therefore, in practice, the correction factor α with CGP 12177 is defined from the blood concentration measured in the cavity ($B_c^*(t)$) and the ligand doses through the following relationship:

$$\alpha = \mu \frac{D_1^* \int_{T_2}^{T_2+\Delta} B_c^*(t)dt}{D_2^* \int_0^{\Delta} B_c^*(t)dt}, \qquad \text{Eq. 5A}$$

where coefficient μ is set at 1.15, as described in the text.

Analytic Calculation of C_1^*. Let us consider the mathematic model shown in Figure 1. Because dissociation of the bound ligand, k_{off} B*(t), can be ignored during the distribution phase (assumption 2), we deduce that the binding kinetics of the labeled ligand during the period [0, Δ] is described by the following equation:

$$\frac{dB^*(t)}{dt} = (k_{on}/V_R)(B'_{max} - B^*(t))F^*(t)$$

$$B^*(0) = 0 \qquad \text{Eq. 6A}$$

This differential equation can be solved analytically. One deduces the concentration of the bound ligand at Δ minutes after the first injection:

$$B^*(\Delta) = B'_{max}(1 - e^{-(k_{on}/V_R)(\int_0^{\Delta} F^*(\tau)d\tau)}). \qquad \text{Eq. 7A}$$

Using Equation 1A and assuming that $C_1^* \approx B^*(\Delta)$ (assumption 1), one deduces that:

$$C_1^* = B'_{max}(1 - e^{-\beta D_1^*}), \qquad \text{Eq. 8A}$$

where

$$\beta = (k_{on}/V_R)\gamma). \qquad \text{Eq. 9A}$$

Observe that, from Equation 8A, we also obtain:

$$\beta = -\left(\frac{1}{D_1^*}\right) \log\left(\frac{B'_{max} - C_1^*}{B'_{max}}\right). \qquad \text{Eq. 10A}$$

Analytic Calculation of C_2^*. At time T_2, a second injection is performed. Assuming that this injection includes both labeled and unlabeled ligand, the binding kinetics of the corresponding labeled ligand during the period [T_2, $T_2 + \Delta$] is described by the following differential equation:

$$\frac{dB^*(t)}{dt} = (k_{on}/V_R)(B'_{max} - C^*(T_2 - \varepsilon) - B^*(t) - B(t))F^*(t)$$

$$B^*(T_2) = 0, \qquad \text{Eq. 11A}$$

where B(t) is the concentration of the bound unlabeled

ligand resulting from the second injection. Because (from the principle of a tracer):

$$B(t) = \frac{D_2}{D_2^*} B^*(t), \qquad \text{Eq. 12A}$$

one obtains the following differential equation:

$$\frac{dB^*(t)}{dt} = (k_{on}/V_R)\left(B'_{max} - C^*(T_2 - \varepsilon) - \left(\frac{D_2 + D_2^*}{D_2^*}\right)B^*(t)\right)F^*(t)$$

$$B^*(T_2) = 0, \qquad \text{Eq. 13A}$$

which gives the solution:

$$B^*(T_2 + \Delta) = (B'_{max} - C^*(T_2 - \varepsilon))\left(\frac{D_2^*}{D_2 + D_2^*}\right)\left(1 - e^{-(k_{on}/V_R)\left(\frac{D_2 + D_2^*}{D_2^*}\right)\left(\int_{T_2}^{T_2+\Delta} F^*(\tau)d\tau\right)}\right). \qquad \text{Eq. 14A}$$

Using Equations 2A and 9A and assuming that $C_2^* \approx B^*(T_2 + \Delta)$ (assumption 1), one obtains:

$$C_2^* = (B'_{max} - C^*(T_2 - \varepsilon))\left(\frac{D_2^*}{D_2 + D_2^*}\right)(1 - e^{-(D_2 + D_2^*)\alpha\beta}). \qquad \text{Eq. 15A}$$

Final Relationship. By substituting β thanks to Equation 10A, one obtains the final relationship:

$$(B'_{max} - C^*_{(T_2 - \varepsilon)})\left(1 - e^{\alpha\left(\frac{D_2 + D_2^*}{D_1^*}\right)\log\left(\frac{B'_{max} - C_1^*}{B'_{max}}\right)}\right) - C_2^* \frac{D_2 + D_2^*}{D_2^*} = 0. \qquad \text{Eq. 16A}$$

In this equation, all values are known except B'_{max}, which appears twice. The unique solution of this equation, which is of the type "$f(B'_{max}) = 0$," can easily be obtained using a numeric or graphic method.

ACKNOWLEDGMENTS

The authors thank the cyclotron and radiochemistry staffs of the Service Hospitalier Frédéric Joliot, as well as Evelyne Meriguet, Daniél Thibaudeau, Laurence Laurier, and Patrick Dodilis for technical assistance.

REFERENCES

1. Fowler MB, Laser JA, Hopkins GL, Minobe W, Bristow MR. Assessment of the β-adrenergic receptor pathway in the intact failing human heart: progressive receptor down-regulation and subsensitivity to agonist response. *Circulation.* 1986;74:1290–1302.
2. Bristow MR, Ginsburg R, Minobe W, et al. Decreased catecholamine sensitivity and β-adrenergic receptor density in failing human heart. *N Engl J Med.* 1982; 307:205–211.
3. Brodde OE. β 1- and β 2-adrenoreceptors in human heart: properties, function, and alterations in chronic heart failure. *Pharmacol Rev.* 1991;43:203–242.
4. Deniss AR, Marsh JD, Quigg RJ, Gordon JB, Coluci WS. β-adrenergic receptor number and adenylate function in denervated transplanted and cardiomyopathic human hearts. *Circulation.* 1989;79:1028–1034.
5. Heyliger CE, Pierce GN, Singal PK, Beamish RE, Dhalla NS. Cardiac α- and β-adrenergic receptor alterations in diabetic cardiomyopathy. *Basic Res Cardiol.* 1982;77:610–618.
6. Staehelin M, Hertel C. [^{3}H]CGP 12177: a β-adrenergic ligand suitable for measuring cell surface receptors. *J Recept Res.* 1983;3:35–43.
7. Staehelin M, Simons P, Jaeggi K, Wigger N. CGP 12177: a hydrophilic β-adrenergic receptor radioligand reveals high affinity binding of antagonist to intact cells. *J Biol Chem.* 1983;258:3496–3502.
8. Hertel C, Müller P, Portenier M, Staehelin M. Determination of the desensitization of β-adrenergic receptors by [^{3}H]CGP 12177. *Biochem J.* 1983;216:669–674.
9. Syrota A. PET: evaluation of cardiac receptors. In: Marcus ML, Skorton HR, Schelbert HR, Wolf GL, Braunwald E, eds. *Cardiac Imaging: Principles and Practice—A Companion of Braunwald's Heart Disease.* Philadelphia, PA: W.B. Saunders; 1990:1256–1270.
10. Delforge J, Syrota A, Mazoyer B. Experimental design optimization: theory and application to estimation of receptor model parameters using dynamic positron emission tomography. *Phys Med Biol.* 1989;34:419–435.
11. Delforge J, Syrota A, Bottlaender M, et al. Modeling analysis of [^{11}C]flumazenil studied by PET: application to a critical study of the equilibrium approaches. *J Cereb Blood Flow Metab.* 1993;13:454–468.
12. Delforge J, Syrota A, Lançon JP, et al. Cardiac β-adrenergic receptor density measured in vivo using PET, CGP 12177 and a new graphical method. *J Nucl Med.* 1991;32:739–748.
13. Delforge J, Le Guludec D, Syrota A, et al. Quantification of myocardial muscarinic receptors with PET in humans. *J Nucl Med.* 1993;34:981–991.
14. Le Guludec D, Delforge J, Syrota A, et al. In vivo quantification of myocardial muscarinic receptors in heart transplant patients. *Circulation.* 1994;99:172–178.
15. Merlet P, Delforge J, Syrota A, et al. PET with C11-CGP 12177 to assess β-adrenergic receptor concentration in idiopathic dilated cardiomyopathy. *Circulation.* 1993;87:1169–1178.
16. De Jong R, Rhodes C, Anthonio R, et al. Parametric polar maps of regional myocardial β-adrenoceptor density. *J Nucl Med.* 1999;40:507–512.
17. Lefroy D, De Silva R, Choudhury L, et al. Diffuse reduction of myocardial β-adrenoceptor in hypertrophic cardiomyopathy: a study with PET. *J Am Coll Cardiol.* 1993;22:1653–1660.
18. Qing F, Rhodes CG, Hayes MJ, et al. In vivo quantification of human pulmonary β-adrenoceptor density using PET: comparison with in vitro radioligand binding. *J Nucl Med.* 1996;37:1275–1281.
19. Ueki J, Rhodes CG, Hughes JMB, et al. In vivo quantification of pulmonary β-adrenoceptor density in humans with (S)-[^{11}C]CGP-12177 and PET. *J Appl Physiol.* 1993;75:559–565.
20. Hammadi A, Crouzel C. Asymmetric synthesis of (2S)- and (2R)-4-[3-tert-butylamino-2-hydroxypropoxy]benzimidazol-2-[^{11}C]one ((S)- and (R)-[^{11}C]CGP 12177) from optically active precursors. *J Labelled Compds Radiopharm.* 1991; 29:681–690.
21. Landais P, Crouzel C. A new synthesis of ^{11}C labeled phosgene. *Appl Radiat Isot.* 1987;38:297–300.
22. Link JM, Krohn KA. A simplified production of high specific activity [^{11}C]labeled phosgene, $^{11}COCl_2$. *J Labelled Compds Radiopharm.* 1997;40:306–308.
23. *Guide for the Care and Use of Laboratory Animals*. Washington, DC: National Academy Press; 1996.
24. Syrota A, Paillotin G, Davy JM, Aumont MC. Kinetics of in vivo binding of antagonist to muscarinic cholinergic receptor in the human heart studied by PET. *Life Sci.* 1984;35:937–945.
25. Mintun MA, Raichle ME, Kilbourn MR, Wooten GF, Welch MJ. A quantitative model for the in vivo assessment of drug binding sites with PET. *Ann Neurol.* 1984;15:217–227.
26. Huang SC, Barrio JR, Phelps M. Neuroreceptor assay with PET: equilibrium versus dynamic approach. *J Cereb Blood Flow Metab.* 1986;6:515–521.
27. Beck JV, Arnold KJ. *Parameter Estimation in Engineering and Science.* New York, NY: John Wiley and Sons; 1977.
28. Van Waarde A, Anthonio R, Visser T, et al. Quantification of an ^{11}C-labeled β-adrenoceptor ligand S-(-)CGP 12177, in plasma of humans and rats. *J Chromatogr B Biomed Appl.* 1995;663:361–369.
29. Luthra SK, Osman S, Steel CJ, et al. Comparison of S-[^{11}C]CGP 12177 metabolism in rat, dog and man using solid phase extraction and HPLC [abstract]. *J Labelled Compds Radiopharm.* 1993;32:504–505.
30. Stöcklin G, Pike VW, eds. *Radiopharmaceuticals for Positron Emission Tomography: Methodological Aspects.* Dordrecht, Germany: Kluwer Academic Publishers; 1993:151–178.
31. Delforge J, Janier M, Syrota A, et al. Noninvasive quantification of muscarinic receptors in vivo with PET in the dog heart. *Circulation.* 1990;82:1494–1504.
32. Rhodes CG, Hughes JMB. Pulmonary studies using PET. *Eur Respir J.* 1995;8: 1001–1017.